EVS29 Symposium
Montréal, Québec, Canada, June 19 - 22, 2016

A Two-wheel Driven Power Train for Improved Safety and Efficiency in Electric Motorbikes

Matthias Baumann[1], Michael Buchholz[1], Klaus Dietmayer[1]
[1]*Institute of Measurement, Control and Microtechnology, University of Ulm, D-89081 Ulm, Germany,*
e-mail: {matthias.baumann, michael.buchholz, klaus.dietmayer}@uni-ulm.de

Abstract

In this contribution, additional degrees of freedom resulting from an additional motor in the front wheel (all-wheel driven motorbike) are used within newly developed methods for enhancing safety and energy efficiency. All algorithms have been developed with respect to realtime capability on a ECU. The basis of the investigations is a test vehicle based on a commercially available electric moped, whose power train was modified for the research purposes with the support of industry partners.

Keywords: *control system, EV (electric vehicle), motorcycle, power management, regenerative braking*

1 Introduction

The use of all-wheel driven power trains offers additional degrees of freedom within driving dynamics control as well as energy efficient driving. For electric vehicles, the distribution of power to all wheels is relatively easy, since one electric motor per wheel can be used. Especially for motorbikes, an additional electric motor at the front wheel allows for significant recuperation, since most of the braking force is usually applied on the front wheel. In addition, this offers a relatively cheap possibility to realize non-wearing braking even for small motorbikes or mopeds.
In this contribution, the results of a research project mainly funded by the Ministry of Finance and Economics Baden-Württemberg, Germany, are presented, where an all-wheel driven power train for electric motorbikes was developed based on the commercially available electric moped Elmoto HR-2 [6]. The hardware developments have mainly been contributed by the industrial partners ID-BIKE GmbH, Stuttgart; Gigatronik Technologies GmbH, Ulm; and ipdd GmbH & Co. KG, Stuttgart. The developed power train comprises a second motor on the front wheel including the required power electronics, which are connected to the same battery as the usual rear wheel motor. To allow for recuperation, i.e. regaining the braking energy by using the electric motors to decelerate the bike and transforming the braking energy to electric energy, the battery with very limited charging current was extended by additional super capacitors which can handle high peak currents. Also, an electric-mechanical brake was installed for backup if the electric braking torque of the motors is not sufficient. The new power train concept is a

(a) Test vehicle (b) Modified suspension fork

Figure 1: All-wheel driven motorcycle

cost-effective method allowing for recuperative and non-wearing braking within electric motorbikes and mopeds. The test vehicle is presented in detail in Section 2.

The Institute of Measurement, Control and Microtechnology at Ulm University has been responsible for power train control and energy management. Within the project, several model-based methods to supervise and enhance the safety of all-wheel driven motorbikes as well as energy efficient power train control methods have been developed, which are presented in this contribution in Section 3. This comprises the required model-based determination of relevant, but not measured signals, the energy-efficient distribution of load between front and rear wheel also with respect to constraints like maximum tire forces, and the reduction of unwanted effects on the driver like the brake steering torque.

2 All Wheel Driven Motorcycle

In Fig. 1(a), the developed all wheel driven motorcycle is shown. It is based on the commercially available electric moped Elmoto HR-2 [6]. To realize an additional front wheel drive, an original rear wheel including the hub motor was used as a front wheel within an adapted suspension fork (see Fig. 1(b)). This motor is driven by an additional power electronics unit which is also identical in hardware to that for the rear wheel. For supervisory control, a rapid prototyping control unit (dSPACE MicroAutoBox I [4]) was also added to the vehicle.

2.1 Power Train Topology

Fig. 2 illustrates the architecture of the test vehicle schematically. The demanded torque as an analogous signal given by the driver via the rotary handle is converted from the display to a CAN message. The MicroAutoBox (MAB) splits the torque (for more details see Sec. 3) dependent on the actual driving situation and forwards it to the control units. Thereby, the current limits are taken into account. Within the control units (CU), the commutation of the hub motors takes place. Therefore, a field-oriented control has been implemented based on [10] by Gigatronik Technologies. The aim of the FOC is to obtain a decoupled control of magnetic flux and torque. The control structure is shown in Fig. 3. The desired value of the torque generating current i_q^* is set by the MAB, leading to a proportional torque T around the hub motors. In case of braking i_q^* is negative. The recuperated energy is stored in the super capacitors. If these are fully charged, the energy is passed to the charging terminal of the battery within the allowed limits and the rest is dissipated in the braking resistors.

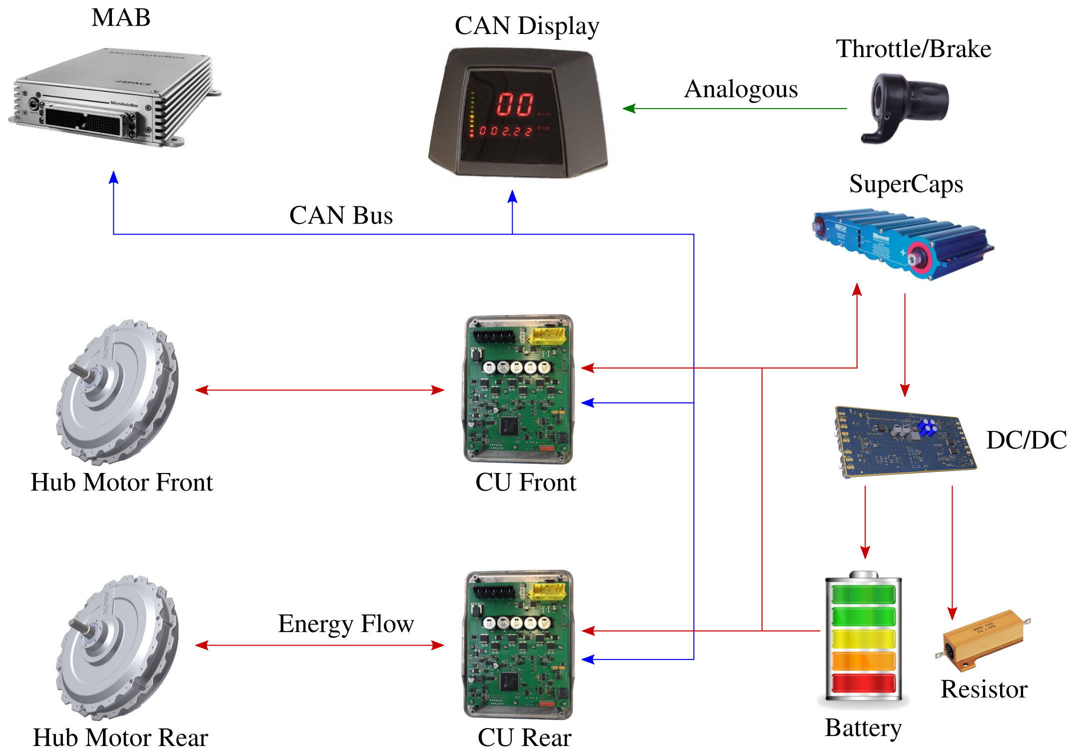

Figure 2: Architecture of the test vehicle

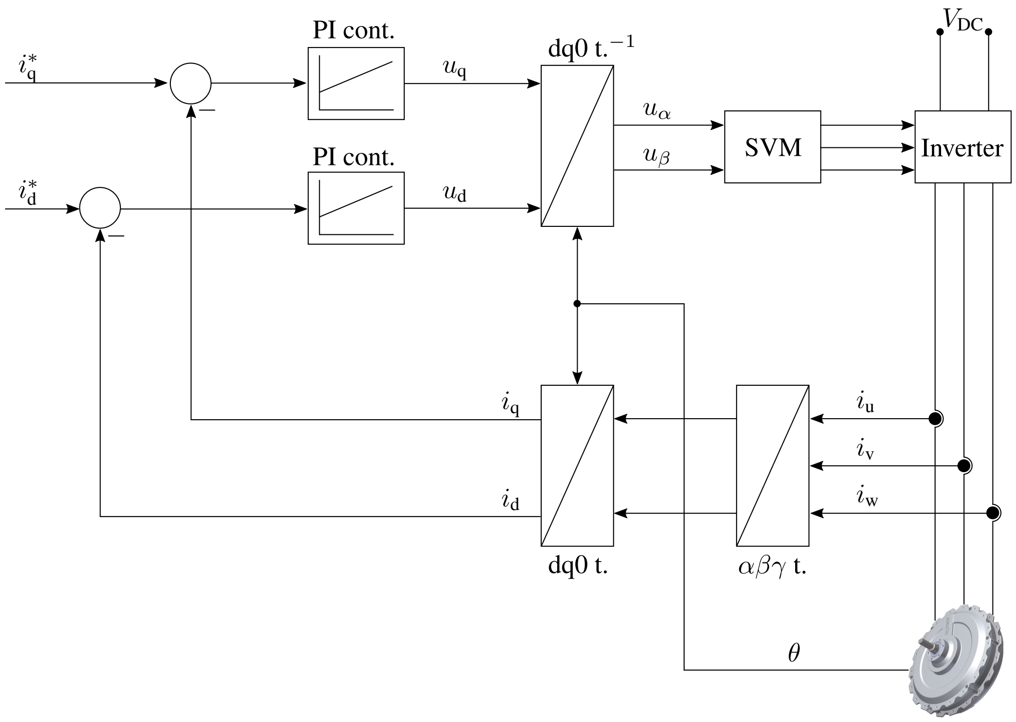

Figure 3: Structure of field-oriented control

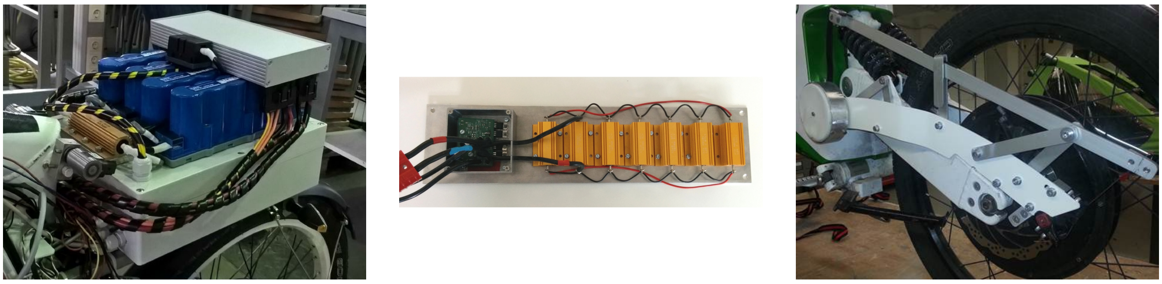

(a) Super capacitors (b) Brake chopper resistor (c) Electric-mechanical brake

Figure 4: Modules of the electric braking system

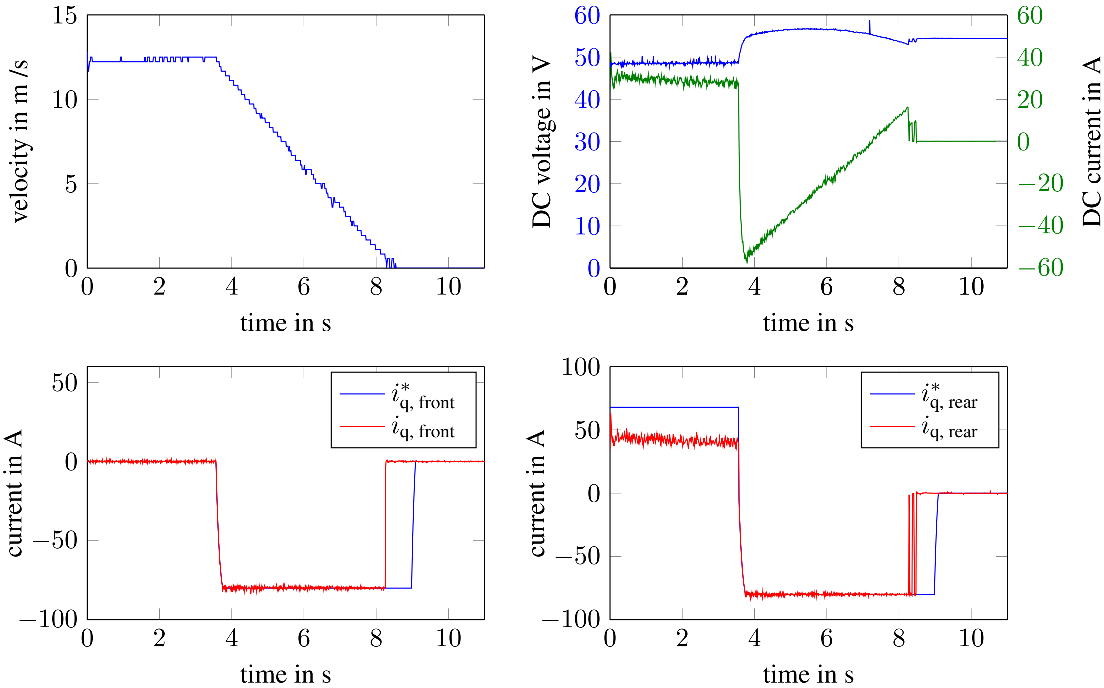

Figure 5: Braking scenario with super capacitor

2.2 Electric Braking System

Since the battery in this vehicle only allows very limited charging currents, the energy storage system had to be extended by a super capacitor module containing a dedicated control unit to realize recuperation capability. The super capacitors have been integrated into the DC voltage circuit of the test vehicle by Gigatronik Technologies. The electric braking system (Fig. 4) additionally comprises of brake chopper resistors also integrated into the DC voltage circuit by Gigatronik Technologies and an electric-mechanical brake using the rear wheel's original brake disc as fallback level provided by ipdd. The operation of the electric braking system in the test vehicle is shown in Fig. 5. The braking maneuver begins at $3.5\,\mathrm{s}$ starting from the maximal permissible velocity $v_0 = 12.5\,\mathrm{m/s}$. Due to the speed restriction, the desired value of $i^*_{\text{q, rear}}$ differs from the actual current $i_{\text{q, rear}}$ before braking. It can be seen that the DC voltage rises and negative DC current occurs. Due to the limited efficiency of the hub motors, the DC current has to be positive to allow the electric braking for low velocities $v < 2.5\,\mathrm{m/s}$. The higher voltage level after braking indicates the stored recuperative energy in the super capacitors. The difference of the desired and actual values of the torque-generating currents after $8.5\,\mathrm{s}$ are because the vehicle's velocity is already $0\,\mathrm{m/s}$.

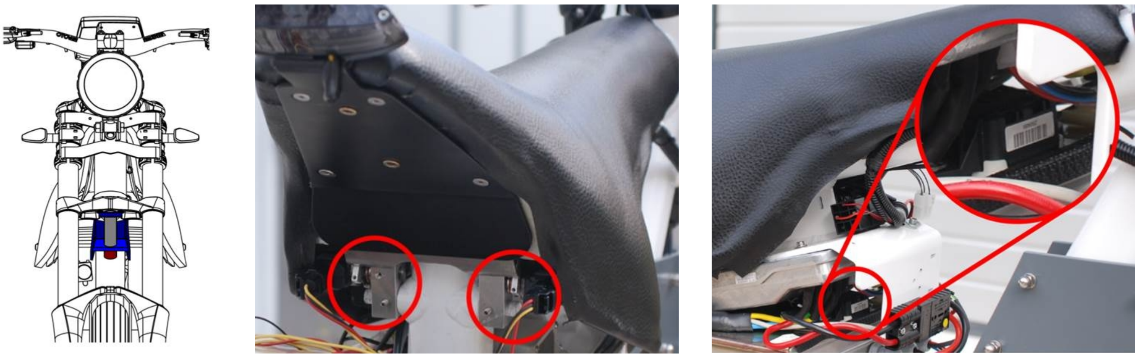

(a) Steering sensor (b) Bosch iBolt (c) Bosch MM5.10

Figure 6: Sensors for vehicle's and driver's state determination

2.3 Sensors

To realize control algorithms assisting the driver, the state of the vehicle has to be monitored. In contrast to cars, the movement of the driver's center of gravity is a main influence used to steer a motorbike. This means that the driver's state is also required and therefore, additional sensors (see Fig. 6) have been included in the test vehicle. These include a contact-less angle sensor for the steering angle, two force sensors (Bosch iBolt, normally used in cars for seat occupancy detection) for the driver's upper body movement, and an off-the-shelf motorbike sensor (Bosch MM5.10) for accelerations and turning rates.

3 Operational Strategy

In this section, the operational strategies for all wheel driven motorcycles are proposed. The sections 3.3 and 3.4 are based on simulated data gained from the proprietary motorcycle simulation software IPG MotorcycleMaker [7]. Section 3.2 shows measured data from the presented test vehicle. As a basis for the torque distribution, a vehicle's and driver's state determination is required, which is presented in Section 3.1.

3.1 State Estimation

Based on the measured signals of the power train and the signals from the additional sensors presented in Section 2.3, the required information on the actual vehicle's and driver's state is gathered within a Kalman filter. In addition to an improvement of the measured signals, the roll angle is estimated by the filter based on these measurements and an appropriate dynamic model. This determination of the driving situation is used as a basis for the subsequently described operational strategy.

3.2 Efficiency-based Torque Distribution

To improve the range of the test vehicle a torque distribution based on a typical efficiency map for permanent magnet synchronous motors is implemented. The aim is to reduce the power losses in the hub motors. These are defined as

$$P_{\text{loss}} = \sum_i T_{\text{act},\,i}\,\omega_i\,\frac{1-\eta_i\left(T_{\text{act},\,i},\,\omega_i\right)}{\eta_i\left(T_{\text{act},\,i},\,\omega_i\right)}, \quad i \in \{\text{front}, \text{rear}\}\,, \tag{1}$$

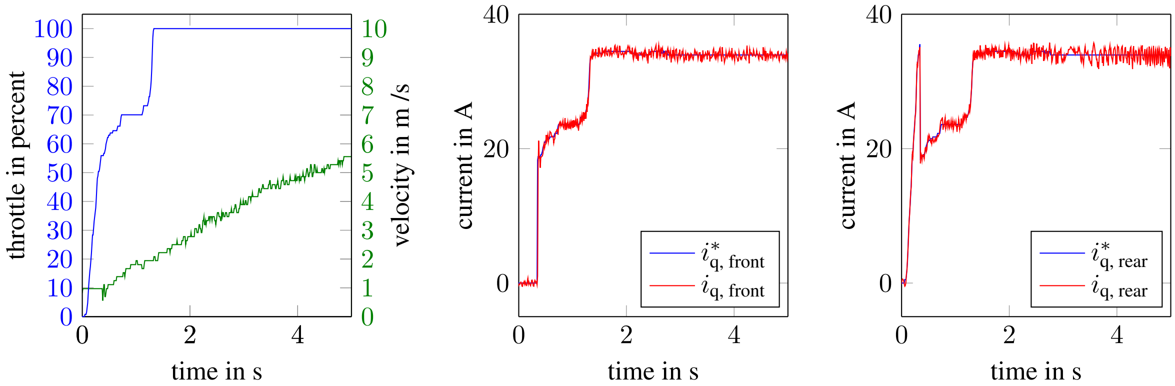

Figure 7: Efficiency-based torque distribution

where $T_{\text{act, }i}$ is the actual applied torque, ω_i the rotational speed and $\eta_i\,(T_{\text{act, }i},\,\omega_i)$ the actual efficiency. The sum of the actual torques leads to the desired torque requested by the driver:

$$T_{\text{des}} = T_{\text{act, front}} + T_{\text{act, rear}}. \tag{2}$$

For different desired torques and rotational velocities, the problem is solved off-line and the calculated optimal torque distribution is stored as a look-up table in the MAB. Dependent on the demanded torque and the actual rotational velocities, a torque distribution is executed. In Fig. 7, an acceleration process is shown. The demanded torque given by the driver and the actual velocity are demonstrated. It can be seen that the demanded torque in the beginning is provided by the rear propulsion unit solely, because the rear wheel is intentionally favorred to avoid ambiguousness and provide a more usual driving experience. Then, from a certain point, both propulsion units provide the required torque, since this allocation is more efficient.

3.3 Model Predictive Control Allocation

The MPCA is based on a method first presented for electric cars [1], which was adapted for the motorbike application. The underlying motorbike model was derived based on the model described in [12], which has been adapted to fit the application with respect to structure, parameters, available measurements, and calculation times [2]. The aim is to reduce the unwanted brake steer torque (BST) [12], which occurs while braking in a cornering situation. In the following, the relevant system equations will be defined. Detailed information on the derivation of this method can be found in [2]. The hub motors are modeled as first-order lag elements with unity stationary gain and time constant T_{m}. The state-space representation of the actuator model is given by

$$\dot{\boldsymbol{x}} = \begin{bmatrix} -\frac{1}{T_{\text{m}}} & 0 \\ 0 & -\frac{1}{T_{\text{m}}} \end{bmatrix} \boldsymbol{x} + \begin{bmatrix} \frac{1}{T_{\text{m}}} & 0 \\ 0 & \frac{1}{T_{\text{m}}} \end{bmatrix} \boldsymbol{u}, \quad \boldsymbol{y} = \begin{bmatrix} 1 & 0 \\ 0 & 1 \end{bmatrix} \boldsymbol{x}, \tag{3}$$

where the state $\boldsymbol{x} = [T_{\text{act, front}}, T_{\text{act, rear}}]^{\text{T}}$ contains the actual torques and the input comprises the desired torques $\boldsymbol{u} = [T_{\text{des, front}}, T_{\text{des, rear}}]^{\text{T}}$. In the following, it is written in the general form

$$\dot{\boldsymbol{x}} = \boldsymbol{f}(\boldsymbol{x},\,\boldsymbol{u}). \tag{4}$$

The BST can be written as

$$T_\delta = \left(\frac{x_1}{r_{\text{front}}} r_{\text{front, c}} \sin\lambda_{\text{front}} + \frac{x_2}{r_{\text{rear}}} r_{\text{rear, c}} \sin\lambda_{\text{rear}} \frac{a}{a+p} \right) \cos\epsilon\,, \tag{5}$$

where r_i is the radius of the tire and $r_{i,\,\mathrm{c}}$ is the radius of the tire cross section. The caster angle of the motorcycle is given by ϵ. The distance between the tire contact points is given by the wheelbase p and the trail a describes the horizontal distance between the front tire contact point and the point where the steering axis intersects the ground. The roll angle of a tire is denoted by λ_i.
To reduce the surprise effect for the driver, the change rate of the BST is taken into account. It can be approximated by

$$\dot{T}_\delta \approx \left(\frac{\dot{x}_1}{r_\mathrm{front}} r_\mathrm{front,\,c} \sin \lambda_\mathrm{front} + \frac{\dot{x}_2}{r_\mathrm{rear}} r_\mathrm{rear,\,c} \sin \lambda_\mathrm{rear} \frac{a}{a+p} \right) \cos \epsilon \,. \tag{6}$$

The resulting longitudinal force is given as

$$F_x \approx \frac{T_\mathrm{act,\,rear}}{r_\mathrm{rear}} + \frac{T_\mathrm{act,\,front}}{r_\mathrm{front}} \cos \delta_\mathrm{kin}, \tag{7}$$

with the kinematic steering angle

$$\delta_\mathrm{kin} = \arctan \left(\frac{\sin\delta \cos\epsilon}{\cos\phi \cos\delta - \sin\phi \sin\delta \sin\epsilon} \right). \tag{8}$$

The motorcycle's steering angle and the roll angle are denoted by δ and ϕ, respectively.
Using these equations, the following optimal control problem (OCP) can be set up:

$$\begin{aligned} \min_{\bar{\boldsymbol{u}}(t)} \quad & J(\boldsymbol{x}_k, \bar{\boldsymbol{u}}) = \int_{t_k}^{t_k+T} l(\bar{\boldsymbol{x}}(t), \bar{\boldsymbol{u}}(t)) dt \qquad (9) \\ s.t. \quad & \dot{\bar{\boldsymbol{x}}}(t) = \boldsymbol{f}(\bar{\boldsymbol{x}}, \bar{\boldsymbol{u}}), \bar{\boldsymbol{x}}(t_k) = \boldsymbol{x}_k, \\ & \bar{u}_i(t) \in [T^-_{\mathrm{des},\,i}, T^+_{\mathrm{des},\,i}], \quad i \in \{\mathrm{front}, \mathrm{rear}\}\,, \end{aligned}$$

where T is the prediction horizon and the cost functional is given by

$$\begin{aligned} l(\boldsymbol{x}, \boldsymbol{u}) = {} & (\boldsymbol{x} - \hat{\boldsymbol{x}})^\mathrm{T} \boldsymbol{Q} (\boldsymbol{x} - \hat{\boldsymbol{x}}) + \boldsymbol{u}^\mathrm{T} \boldsymbol{R} \boldsymbol{u} \\ & + \gamma_1 T_\delta^2 + \gamma_2 \dot{T}_\delta^2 + \gamma_3 (F_x - F_{\mathrm{des},x})^2 \,. \end{aligned} \tag{10}$$

The limits for the input are given by $T^-_{\mathrm{des},\,i}$ and $T^+_{\mathrm{des},\,i}$. Using the factors γ_1, γ_2, γ_3, the different goals can be weighted. The matrix $\boldsymbol{R}$ weights the usage of the inputs and the matrix $\boldsymbol{Q}$ penalizes the difference to the pre-allocated states. The OCP can be solved on-line with the open-source software GRAMPC [9] within the given limits for the acting torques.
Simulation results are shown in Fig. 8. Here, the driver suddenly brakes during a constant circular drive. In Fig. 8(a), the longitudinal forces at the wheels are presented. The blue lines show a conventional braking method, where the braking force mainly is applied at the front wheel, and the red lines represent the forces calculated with the MPCA algorithm. In Fig. 8(b), it can be seen that the driver's steering torque is significantly reduced by the MPCA algorithm.

3.4 Traction Control

Based on [3], the idea for a traction control (TC) is to observe the angular accelerations of the wheels and keep them limited. If their magnitude become too large, then the limits for the applied torques in the MPCA algorithm are reduced. After the longitudinal slip returned into the stable region, the limits are increased again. To detect the critical angular accelerations a Kalman filter is used. First, the system modeling is described. The wheel dynamics are modeled according to [8] as follows:

$$\dot{\omega}_i = -\frac{r_i}{J_i} F_{x,i} + \frac{1}{J_i} T_{\mathrm{act},\,i}\,, \qquad i \in \{\mathrm{front}, \mathrm{rear}\}, \tag{11}$$

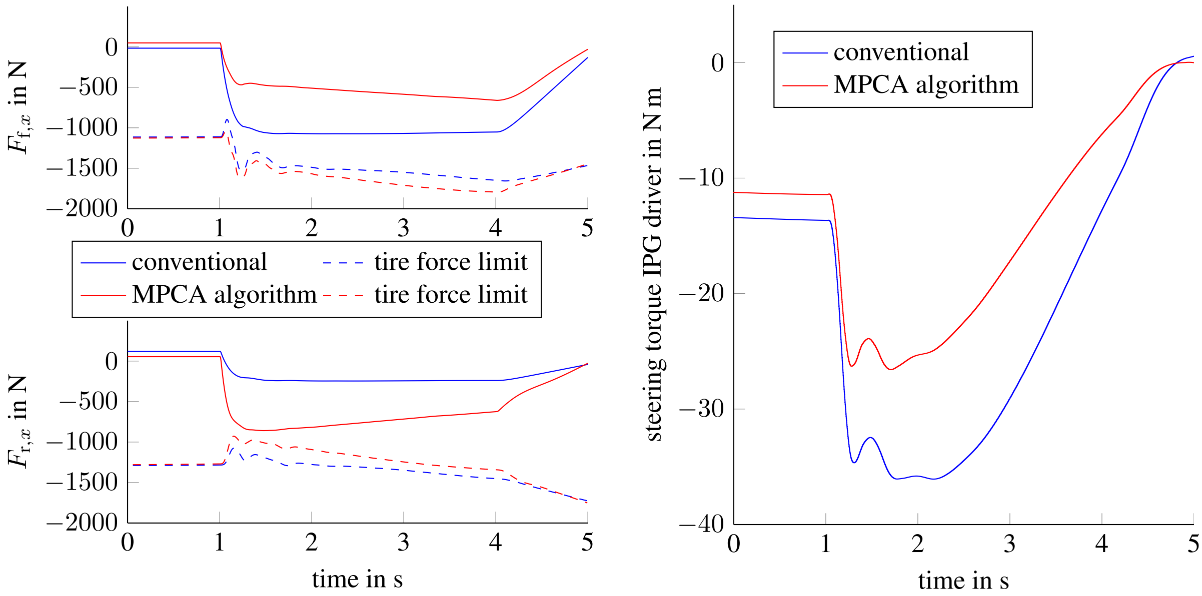

(a) Force distribution

(b) Driver's steering torque

Figure 8: Reducing the brake steer torque (for detailed information see [2])

where J_i is the moment of inertia of each wheel. For the longitudinal forces, an integrator disturbance model is assumed:

$$\dot{F}_{x,i} = 0\,, \qquad i \in \{\text{front, rear}\}. \tag{12}$$

The rotation angles are measured using the hall sensors installed in the hub motors. Thereby, the system output is defined as follows:

$$y_i = \theta_i\,, \qquad i \in \{\text{front, rear}\}. \tag{13}$$

The sensors update every 3 ms with a resolution of 138 readings per rotation. This set-up is also implemented in the simulation scenario.
Choosing the state space vector as $\boldsymbol{x} = [\theta_{\text{front}}, \omega_{\text{front}}, \theta_{\text{rear}}, \omega_{\text{rear}}, F_{x,\text{front}}, F_{x,\text{rear}}]^{\mathrm{T}}$ and the control vector as $\boldsymbol{u} = [T_{\text{act, front}}, T_{\text{act, rear}}]^{\mathrm{T}}$, this leads to the following state space representation:

$$\dot{\boldsymbol{x}} = \boldsymbol{f}(\boldsymbol{x}, \boldsymbol{u}), \tag{14}$$
$$\boldsymbol{y} = \boldsymbol{h}(\boldsymbol{x}). \tag{15}$$

The aim is to observe the state space vector and then calculate the rotation accelerations. For this task, a central difference Kalman filter (CDKF) based on [5] is used, which is from the class of sigma point Kalman filters (for a detailed derivation see [11]).
The operation of the traction control is demonstrated in Fig. 9. A braking maneuver while driving straight ahead with a sudden decrease of the friction coefficient is simulated. It can be seen that without the traction control, the magnitudes of angular accelerations are getting very high (green lines). Thereby, the slips leave the stable area (dotted lines), so an accident is the possible consequence. If the traction control is active, the blue lines are the angular accelerations from the simulation environment the and red lines are the estimations using the described method. The limits for the input of the MPCA are restricted when the magnitudes of the estimated angular accelerations exceed a threshold and slowly released after a while. Hereby, the longitudinal slips remain in the stable region and a secure operation can be ensured.

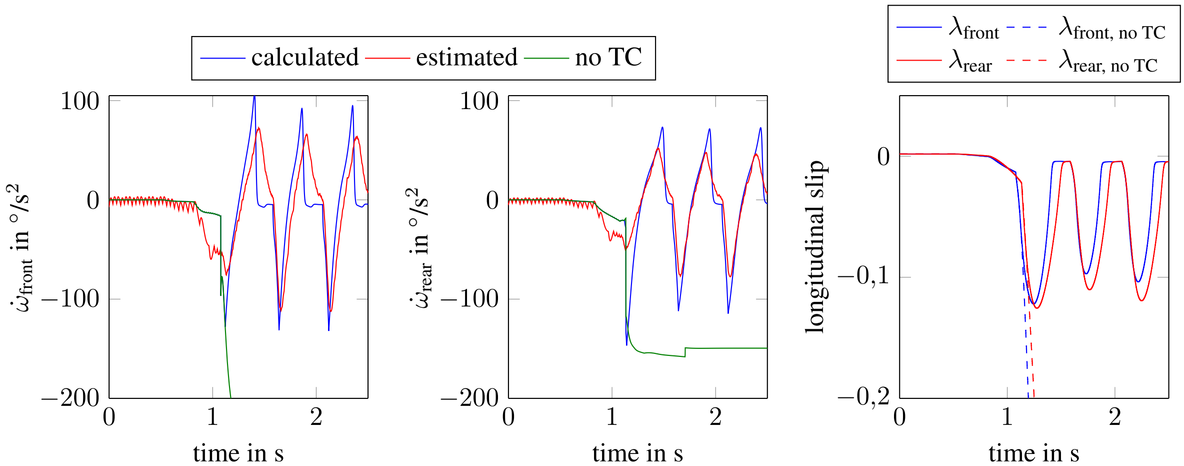

Figure 9: Traction Control

4 Conclusion

In this contribution, the operational strategy for an all wheel driven electric motorcycle was presented together with an description of the underlying test vehicle, which now allows for recuperation. As a basis, the required state information of the vehicle and the driver are gained by additional sensors and a Kalman filter. An efficiency based torque distribution that splits the demanded torque dependent on an efficiency map has been introduced as base strategy. Additionally, a much more sophisticated model predictive control algorithm for reducing the unwanted brake steer torque while braking in a corner by adaptive distribution of the torques has been demonstrated. Finally, a traction control approach for increasing the safety based on the observation of the rotational accelerations of the wheels and the limitation of the desired torques was presented and discussed. Overall, it could be shown that the additional degree of freedom of an added front wheel drive enables for enhanced safety and efficiency in electric motorcycle control by relatively simple and therefore easily realizable means.

Acknowledgments

The authors would like to thank the Ministry of Finance and Economics Baden-Württemberg, Germany as well as the industry partners ID-BIKE GmbH, Stuttgart, Gigatronik Technologies GmbH, Ulm, ipdd GmbH & Co.KG, Stuttgart, for funding and supporting this project.

References

[1] Thomas Bächle, Knut Graichen, Michael Buchholz, and Klaus Dietmayer. Model predictive control allocation in electric vehicle drive trains. *IFAC-PapersOnLine*, 48(15):335 – 340, 2015. 4th IFAC Workshop on Engine and Powertrain Control, Simulation and Modeling, E-COSM 2015, Columbus, Ohio, USA, 23-26 August 2015.

[2] Matthias Baumann, Thomas Bächle, Michael Buchholz, and Klaus Dietmayer. Model-based corner braking control for electric motorcycles. 8th IFAC Symposium on Advances in Automotive Control - AAC 2016, Kolmården Wildlife Resort, Sweden, 20-23 June 2016, accepted.

[3] Manfred Burckhardt. *Fahrwerktechnik: Radschlupf-Regelsysteme*. Vogel-Verlag, 1993.

[4] dSPACE GmbH. MicroAutoBox. `https://www.dspace.com/de/gmb/home.cfm`, accessed on 2016-03-15.

[5] Joachim Fox. *Robotergestützte Parameterschätzung für inertiale Messsysteme*. Logos, 2007.

[6] ID-BIKE GmbH. Elmoto. `http://www.elmoto.com/`, accessed on 2016-03-15.

[7] IPG Automotive GmbH. IPG MotorcycleMaker. `http://www.ipg.de/en/simulation-software/motorcyclemaker/`, accessed on 2016-03-15.

[8] Rolf Isermann. *Fahrdynamik-Regelung: Modellbildung, Fahrerassistenzsysteme, Mechatronik*. Springer-Verlag, 2007.

[9] Bartosz Käpernick and Knut Graichen. The gradient based nonlinear model predictive control software GRAMPC. In *European Control Conference (ECC)*, pages 1170–1175. IEEE, 2014.

[10] Bassel Sahhary. *Elektrische Antriebe mit dauermagneterregten Maschinen im dynamischen sensorlosen Betrieb*. PhD thesis, Fakultät für Elektrotechnik der Helmut-Schmidt-Universität, Universität der Bundeswehr Hamburg, 2008.

[11] Rudolph van der Merwe. *Sigma-point Kalman filters for probabilistic inference in dynamic state-space models*. PhD thesis, Oregon Health & Science University, 2004.

[12] A. Weidele. *Untersuchungen zum Bremsverhalten von Motorrädern unter besonderer Berücksichtigung der ABS-geregelten Kurvenbremsung*. Berichte aus dem Fachgebiet Fahrzeugtechnik der TH Darmstadt. VDI-Verlag, 1994.

Authors

Matthias Baumann, M.Sc., received his master's degree in Communications and Computer Engineering from Ulm University in 2013. Since 2013, he is a researcher at the Institute of Measurement, Control, and Microtechnology at Ulm University, working towards his Ph.D. degree in the field of Electric Mobility.

Dr.-Ing. Michael Buchholz received his diploma degree in Electrical Engineering and Information Technology as well as his Ph.D. degree from University of Karlsruhe/Karlsruhe Institute of Technology in 2004 and 2010, respectively. Since 2009, he has been serving as a group leader and lecturer at the Institute of Measurement, Control, and Microtechnology at Ulm University. His main research interests comprise system identification and diagnosis, electric mobility, and mechatronical systems.

Prof. Dr.-Ing. Klaus Dietmayer is director of the Institute of Measurement, Control, and Microtechnology at Ulm University and head of driveU. His main research interests are information fusion, classification methods, stochastic filters and tracking, signal processing, and dynamical modeling and control within automotive applications.